Journal of Applied Polymer Science

Sorption behavior of reactive dyed labelled fibroin on fibrous substrates

Ha-Thanh Ngo, Thomas Bechtold
Research Institute of Textile Chemistry and Textile Physics, Faculty of Chemistry and Pharmacy, Leopold Franzens-Univeristy of Innsbruck, Hoechsterstraße 73, Dornbirn, A-6850, Austria
Correspondence to: T. Bechtold (E-mail: Thomas.Bechtold@uibk.ac.at)

ABSTRACT: Through its biocompatibility, fibroin is of high interest as a material in medical and pharmaceutical applications. Shaping by dissolution in concentrated salt solutions e.g., calcium chloride/ethanol/water and regeneration include structure formation through coagulation, crystallization, and deposition of Ca-complexes. To facilitate analytical monitoring of fibroin during the dissolution and regeneration, fibroin was marked by covalently bound reactive dyes. Fibroin dyed by the mono-functional CI Reactive Blue 19 dissolved completely, the bifunctional CI Reactive Black 5 formed crosslinks between protein chains, thus only fiber swelling was observed. The CI Reactive Blue 19 labelled fibroin was used to monitor the sorption and deposition of fibroin on textile fibers polyamide 6.6, polyester and viscose. The results indicated a temperature and pH-dependent sorption behavior. The highest sorption was observed on polyamide at pH 3 and 60 °C. Dye marked fibroin allows a simple assessment and optimization of regeneration processes for the coating of textile substrates. © 2016 Wiley Periodicals, Inc. J. Appl. Polym. Sci. **2016**, *133*, 43880.

KEYWORDS: biopolymers and renewable polymers; coatings; dyes/pigments; fibers; textiles

Received 10 March 2016; accepted 29 April 2016
DOI: 10.1002/app.43880

INTRODUCTION

Silk has been used in the textile industry over the past 5000 years. Silk fibers exhibit high tensile strength, elasticity, resilience and wrinkle recovery as the fibers are built from clusters of fibrils, which are orderly arranged and oriented along the fiber axis.[1–3] Through its high bio-compatibility and the mechanical robustness of fibroin based materials, it has been widely studied as a bio-material for tissue engineering and regenerative medicine,[4,5] fracture fixation,[6] healing critical sized femur defects,[7,8] bone repair,[9,10] vascular prostheses and structural implants,[11] including possible use as a coating material for controlled drug release.[12] Also application in opto-electronic and photonics technologies has been proposed in the literature.[10] Dissolution and regeneration of the fibroin form the central steps to shape the polymer for different functional applications. Through its solubility in a concentrated salt solution e.g., calcium chloride/water/ethanol (CWE) fibroin can be shaped into multiple material formats such as microphones, gels, sponges, fibers, films, fiber coating.[13,14] CWE is widely used as solvent system,[15–20] regeneration is then achieved by salt removal through dialysis and addition of a non solvent for fibroin e.g., methanol or water.[3,21–24] Also electrogelation, gelation under high shear rate and osmotic gradients have been used for fibroin regeneration.[25,26]

As a protein fiber, silk exhibits a high number of polar groups, e.g., hydroxyl groups, amino groups, and salt bridges which can be utilized to bind dyestuff, thus fibroin can be dyed with a number of different dyes.[13,15] Important classes of dyes include anionic acid dyes and metal complex dyes, as well as direct dyes, which bind to the silk through salt bridges and hydrogen bonds. The fixation of reactive dyes on the fibroin proceeds through formation of a covalent bond. Depending on the number of reactive anchors present in the reactive dye molecule, a distinction is drawn between monofunctional and bifunctional reactive dyes. In the case both anchor groups react with the protein structure, the dyestuff fixation will result in formation of crosslinks between protein chains, while monofunctional dyes will be bound to one chain through the single anchor group present.

In case both anchor groups of a bifunctional reactive dye link to different fibroin chains, the dissolution behavior of fibroin in CWE will change due to presence of crosslinks. Additionally the

Additional Supporting Information may be found in the online version of this article.

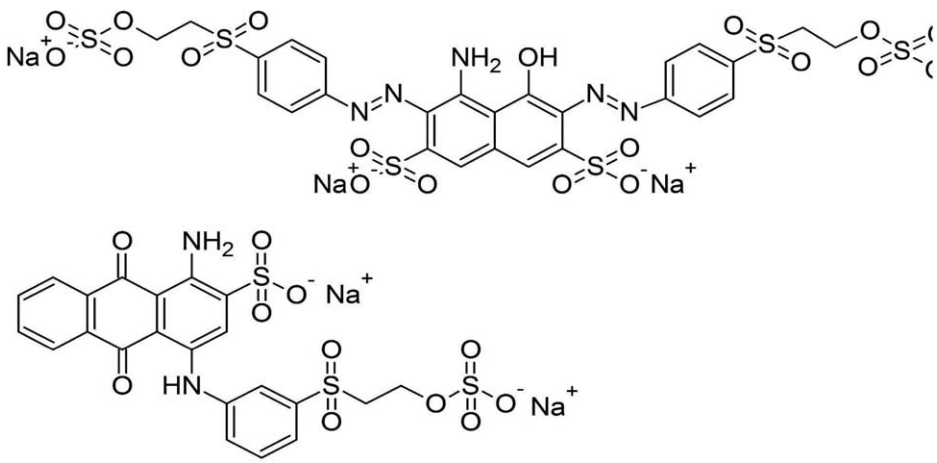

Figure 1. The chemical structures of Reactive Blue 19 (RB19, top) and Reactive Black 5 (RB5, bottom).

use of reactive dyed fibroin could allow for simple monitoring of regeneration processes and sorption studies, as direct photometry can be applied to trace the dyed fibroin.

In this research, the modification of the fibroin structure and solubility in CWE after treatment with two different reactive dyes, the mono-functional Reactive Blue 19 (RB19) and the bifunctional Reactive Black 5 (RB5) (Figure 1) as investigated.

Differences in the dissolution behavior of dyed fibroin in CWE (1:8:2 moles) were investigated. The regenerated fibroin was characterized by FTIR, optical microscopy and determination of mass balances. Deposition of the dye marked fibroin from diluted CWE solution was studied on several man-made fibers: polyamide 6.6 (PA), polyester (PES) and viscose (CV) as a function of process conditions temperature and pH. The modified fiber material was characterized by CIELab color measurement, FTIR-ATR spectra and stained by the protein reagent Coomassie Blue G-250. The fibroin content in the treatment solutions was analyzed by photometry. The results open a new way to control the processing and regeneration step of fibroin and also indicate a new approach to modify textile fiber surfaces using fibroin solution.

EXPERIMENTAL

Materials and Chemicals

Silk hanks (Nha Xa textile village, Ha Nam province, Vietnam) were degummed in a solution of 5 g L^{-1} Na_2CO_3 at 95 °C for 60 min at a liquor ratio of 1:100 (mass in g per volume in mL). The material was rinsed five times for 20 min in 500 mL of warm and cold deionized water, and dried at ambient temperature and stored at 65% relative humidity and 20 °C.

Fibers used for sorption experiments were man-made fibers: Viscose (CV, 1.7 dtex, in form of a 150 ktex cable, 1.7/150 GL Kelheim Fibres GmbH, Germany), polyester (PES, 1.3 dtex staple fiber, Spinnerei Feldkirch, Feldkirch, Austria), polyamide 6.6 (PA, 1.7 dtex staple fiber, Spinnerei Feldkirch, Feldkirch, Austria). To remove any chemical residue from the pre-spinning processing, the fibers were washed using a solution of 1 g L^{-1} nonionic detergent (Kieralon B hochkonz., BASF, Ludwigshafen), 1 g L^{-1} Na_2CO_3 at 60 °C for 1 h at a liquor ratio of 1:50. Samples were then rinsed three times with deionized water at room temperature for 10 min, dried at 60 °C and stored under normal climate conditions.

Na_2CO_3 (Merck, Darmstadt, Germany); $CaCl_2.2H_2O$ (Fluka, Buchs, CH); Ethanol (BVDA, Bureau voor Dactyloscopische Artikelen, Haarlem, Holland); methanol, calcium carbonate, (Zeller GmbH, Hohenems, Austria); acetic acid, NaCl, H_3PO_4, NaOH, HCl (Carl Roth GmbH, Karlsruhe, Germany), were analytical grade chemicals. Nonionic detergent (Kieralon B Hochkonz., BASF AG Ludwigshafen, Germany). CI Reactive Blue 19 (RB19, Remazol Brilliant Blue R, dye content ca. 50%) and CI Reactive Black 5 (RB5, Remazol Black B, dye content ca. 55 wt %) were supplied by Sigma–Aldrich (Buchs, Switzerland). Coomassie Blue G-250 was supplied by Fluka (Buchs, Switzerland).

Reactive Dyeing of Fibroin

A mass of 2 g degummed silk was dyed with a reactive dye using an isothermal exhaust dyeing process and a volume of 100 ml dye bath (LR = 1:50). The bath containing 50 mL water and 3 g L^{-1} sodium chloride was heated up to 50 °C. The sample (2 g) was placed in the solution and after 10 min of soaking a solution of 0.16 g dye stuff in 50 mL water was added in three equal portions within 15 min. Then 10 mL sodium carbonate solution (3 g L^{-1}) was added in three equal parts within 30 min. After complete addition of the alkali, the bath temperature was maintained at 50 °C for 30 min for dyestuff fixation. Samples were then rinsed twice with 100 mL tap water for 10 min at 50 °C, followed by a rinse with 100 mL tap water at 70 °C for 10 min and a final rinse with cold tap water. A diagram of the process is shown in Figure 2. The dyed samples were dried at ambient air temperature.

Dissolution and Regeneration of Fibroin

A CWE solution with a molar ratio of 1:8:2 (calcium chloride: water: ethanol) was used as a solvent for fibroin. To prepare the solvent 9.31 g of $CaCl_2.2H_2O$ was dissolved in 6.85 g distilled water and 5.84 g ethanol was added. Fibroin solutions of RB19 or RB5 dyed fibroin were prepared by dissolving 1 g or 1.5 g dyed fibroin in 10 g CWE at 60 °C for 2 h to obtain a solution of 9.1 wt % or 13 wt % fibroin in CWE.

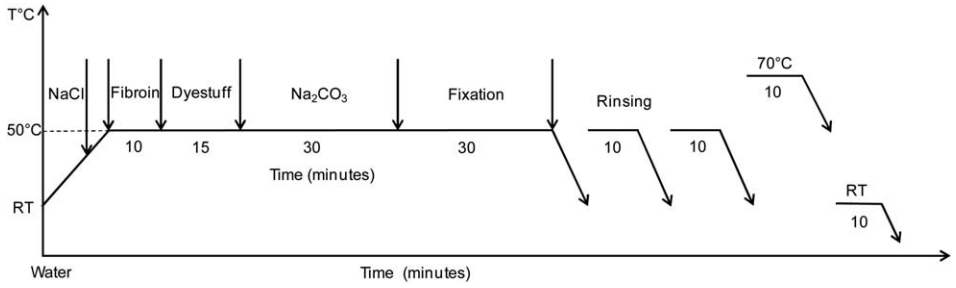

Figure 2. Dyeing diagram for exhaust dyeing of fibroin with reactive dye.

For 11 g of 9.1 wt % fibroin solution in CWE a volume of 50 mL methanol was used to regenerate dissolved RB19 dyed fibroin. Addition of methanol was made in five portions of 10 mL. The solution was agitated in between each addition of methanol and then was kept to rest overnight to allow the regenerated fibroin to coagulate and settle. The regenerated fibroin appeared as a colored sticky substance adhering to the glass walls of the bottle and partly dispersed in the solution. The solution then was removed and filtered by a vacuum using a cellulose-acetate filter (Pore size 0.45 µm, Sartorius AG, Germany). The residues in the bottle were first washed with 10 mL methanol, followed by a rinse with 50 mL deionized water. All solutions were filtered to collect any dispersed regenerated fibroin.

Sorption Experiments

To study the sorption behavior of RB19 marked fibroin on the manmade fibers an exact amount of 13 wt % RB19 dyed fibroin solution in CWE (0, 0.10, 0.20, 0.30, 0.50, 0.70 g) was diluted with 100 mL deionized water (solution S). For experiments at pH 3, the solution was adjusted to pH 3 by the addition of acid acetic 0.5 g of fiber was then immersed into the correct solution and the sorption experiments were continued at 30 °C or 60 °C for 20–24 h. The fibers were then rinsed by 50 mL deionized water three times and dried at 60 °C.

Analytical Methods

Microphotographs and Infrared Spectroscopy. Optical microscopy was used to monitor degummed dyed fibroin during the dissolution process, to analyze solubility of the dyed fibroin (RB5 and RB19) and to observe regenerated fibroin.

The attenuated total reflectance (ATR) of untreated and treated samples was recorded in the spectral range of 4000 to 400 cm^{-1} with a resolution of 1 cm^{-1} and 128 scans using a FTIR-spectrometer (Bruker Vector 22 FTIR Spectrometer). The ATR stage was equipped with a diamond crystal.

Color Measurement and Photometry. To determine the CIELab color coordinates of the samples, a Konica Minolta Spectrophotometer CM 3610d and Spectra Magic Software, d:8° geometry) was used and the coordinates were calculated for D65 illumination. In the CIELab coordinates the L^* is the degree of lightness: 0 for perfect black and 100 for perfect white. The a^* axis represents the position on the red–green axis with positive values for red color and negative values for green color. The b^* axis describes the position on the yellow–blue axis, a positive b value indicates yellow color and a negative value indicates blue color. In addition to the reflectance curves, the K/S values were calculated according to the relation of Kubelka and Munk for the wavelength of maximum absorption. Through a linear relationship between the K/S value and the amount of dye on a substrate, this value permitted the assessment of dyestuff content on the fiber material.

The remaining color of the solution S was analyzed by photometry in a wavelength interval of 400–700 nm using a diode array photometer (Zeiss CLH 500/MCS 521 UV-VIS Carl Zeiss Jena, Jena, Germany).

Protein Staining of Fibroin Treated Fibers. Staining with Coomassie Blue G-250 was used to indicate the presence of fibroin on treated fibers. The reagent solution was prepared by dissolution of 100 mg Coomassie Blue G-250 in 50 mL ethanol (95 wt %), then 100 mL H_3PO_4 (85 w/v %) was added. The solution was filtered through a Whatman #1 paper filter just before use. A volume of 5 mL protein reagent was used to treat 10 mg of fibers for 5 min at ambient temperature in absence of light. The samples were then rinsed extensively with deionized water and dried at ambient temperature.

RESULTS AND DISCUSSION

Solubility of Reactive Dyed Fibroin in Calcium Chloride/Water/Ethanol (CWE)

Fibroin was dyed with 2 different reactive dyes (RB19 and RB5) using an exhaust process. Reactive dyes form a covalent bond between the protein structure and the dyestuff. When the fibroin is dissolved in CWE, the dyestuff will remain linked to the protein chain. Color coordinates and weight increase of dyes samples are shown in the supporting information (Supporting Information Table SI). Thus the monitoring of fibroin regeneration from solution and sorption behavior on fibrous structures can be visualized using dyestuff labelled fibroin. The binding of reactive dyes on the fibroin structure however also modifies the solubility of the labelled protein structure.

While RB19 dyed fibroin could be dissolved in CWE completely, RB5 dyed fibroin fibers only displayed extensive swelling of the filaments. Photographs of the solution obtained are given in the supplementary information (Supporting Information Figure S1). A microphotograph of the highly swollen RB5 labelled fibroin in CWE is shown in Figure 3. Through fiber swelling, the diameter of the filaments increased from originally 9–10 µm to 40–67 µm, which corresponds to a diameter increase of four to seven times, and an increase in volume by a factor of 16–49.

Figure 3. Swollen degummed dyed RB5 dyed fibroin in CWE after 2 h at 60 °C (scale bar 100 µm). [Color figure can be viewed in the online issue, which is available at wileyonlinelibrary.com.]

The different dissolution behavior of reactive dyed fibroin can be explained by the crosslinking of protein chains by the bifunctional RB5. Binding of reactive dyes will mainly occur on hydroxyl side groups and basic amino groups present in fibroin. In fibroin, a substantial amount of amino acids offer reactive side groups to react with the vinylsulfone anchor group of the dye e.g., hydroxyl groups in tyrosine (13.2 wt %), serine (1.8 wt %), and amino groups in lysine (0.9 wt %), arginine (0.9 wt %).[27] In case both reactive vinylsulfone groups of RB5 bind to the amino acids of the neighboring fibroin chains a crosslinking of the fibroin will occur. The formation of stable covalent bridges between individual protein chains will prevent the dissolution of RB5 dyed fibroin in CWE. A reaction scheme of the crosslinking is shown in Figure 4.

Similar behavior has already been observed in cellulose fiber chemistry where modification of fiber fibrillation was attributed to the crosslinking of cellulose chains by RB5.[28]

In the case of RB19, only one covalent bond is formed between the dye and a protein chain, thus dissolution of fibroin in CWE is not prevented by the formation of an interlinked molecular network. The presence of dyestuff molecules, which bear charged groups e.g., sulfonate groups will modify the solubility behavior of protein chains, however due to absence of crosslinks, the dissolution in CWE is not prohibited.

Regeneration Experiments

Regeneration of RB19 labelled fibroin from CWE solution was achieved by the direct addition of methanol.[29] The addition of methanol led to coagulation and precipitation of a blue sticky substance, which for the major part, adhered to the glass wall of the bottle.

From the input of RB19 dyed fibroin to dissolution, regeneration and filtering a mass balance through the process was established (Table I). The main part of regenerated fibroin was obtained as a precipitate from the methanol solution (Fraction

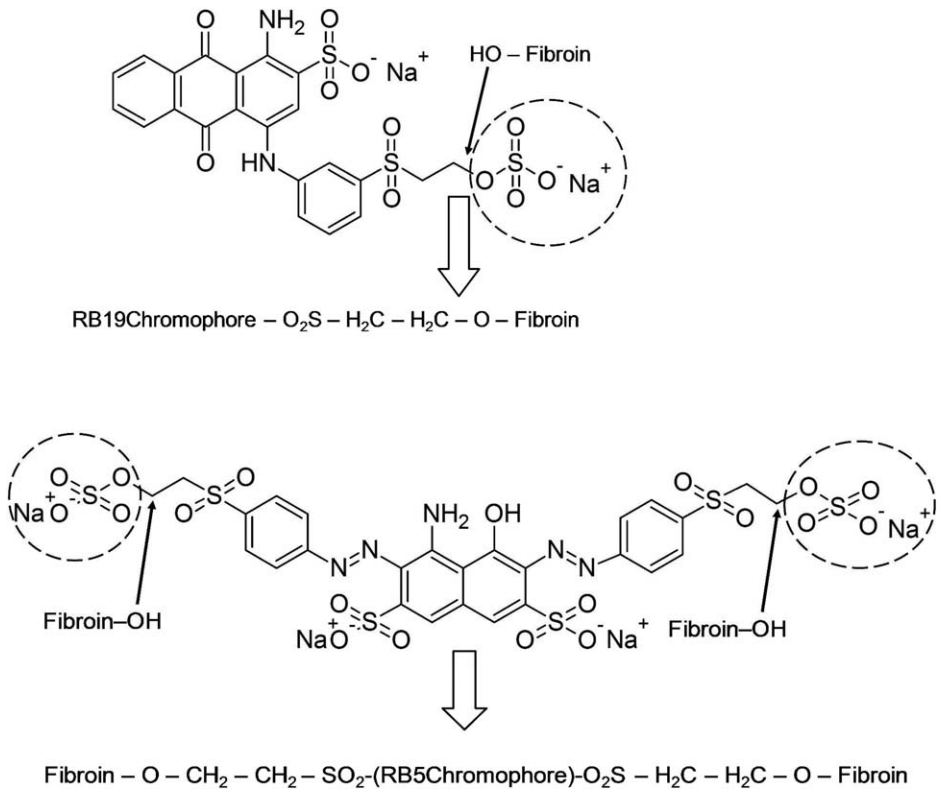

Figure 4. Reaction scheme for fibroin dyeing with RB19 (top) and crosslinking of fibroin due to bond formation of both anchor groups present in RB5 (bottom).

Table I. Mass Balances of Regeneration of RB19 Dyed Fibroin

Experiment no	Dissolved fibroin g	Fraction B g	Fraction F g	Regenerated fibroin g	Yield %
1	1.006	0.972	0.034	1.006	100.0
2	1.000	1.050	0.097	1.147	114.7

B). Another part could be collected by the filtration of the methanol solution (Fraction F).

Two independent experiments were performed and the average yield for regeneration of RB19 dyed fibroin was calculated at 107.4%, indicating that an almost quantitative regeneration was achieved. This matches with the results for regeneration of undyed fibroin from CWE by the addition of methanol, where a Ca-content in the regenerate between 10 and 15 wt % was found, which explained the overall increase in mass of the regenerated fibroin.[29]

The measured absorbance of the methanol filtrates and the aqueous filtrates from the regeneration step also indicated that quantitative regeneration of the dyes silk could be achieved. Absorbance spectra of the filtrates are shown in Figure 5. When a dyestuff fixation of 80% of the 8 wt % dyeing is taken as an estimate, the theoretical maximum dyestuff concentration in the filtrated regeneration solution is calculated with 1066 mg L^{-1} for the methanol solution and 1280 mg L^{-1} for the aqueous solution. From calibration curves performed with the respective reactive dye the actual amount of dye present in the methanol solution was calculated with 1.04 wt % of the total amount for RB19 and 0.55 wt % for RB5. In the aqueous filtrate 0.08 wt % of the dyestuff used was found in the case of RB19, and no residual color was observed for RB5. The results confirm the covalent binding of the reactive dye to the fibroin structure and also indicate complete regeneration of the dyed protein.

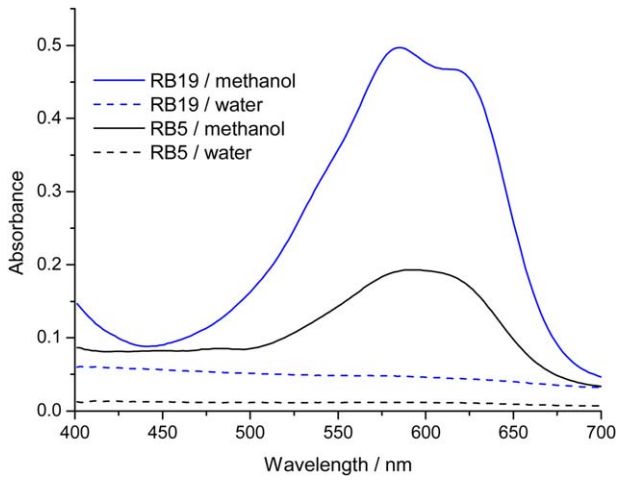

Figure 5. Absorbance curves of the regeneration solutions obtained from RB19 and RB5 dyed fibroin (methanol solution, aqueous solution). [Color figure can be viewed in the online issue, which is available at wileyonlinelibrary.com.]

FTIR-ATR Analysis of RB19 Dyed Fibroin

FTIR spectroscopy was used to identify possible modifications in the protein structure between original and regenerated fibroin samples. FTIR spectra of RB19 dyed fibroin, regenerated undyed fibroin and degummed silk (fibroin) are given in Figure 6.

The amide I region is widely used to evaluate the secondary conformational change in the silk structure. β-sheet conformation is identified by: absorbance in the range of 1616–1637 cm^{-1}; the range of 1638–1655 cm^{-1} is assigned to random coil structure and the absorbance in the interval of 1656–1662 cm^{-1} is attributed to the α-helical conformation. The wavenumber region of 1663–1690 cm^{-1} is attributed to turns structure.[24,30–32] The three characteristic amide I–III bands observed in the FTIR-ATR spectra are presented in Supporting Information Table SII.

Between degummed fibroin, regenerated undyed fibroin and regenerated RB19 labelled fibroin differences in the absorbance spectra can be observed at the Amid I band. Substantial reorganization of the secondary structure of fibroin results from the dissolution and regeneration process, where the presence of Ca-ions will also influence the final conformational structure. Besides β-sheet structure, also significant amounts of random coil and turns structures are detected in the FTIR spectra of regenerated fibroin. From a comparison of the FTIR spectra between labelled and undyed regenerated fibroin, it can be seen, that the amount of dyestuff bound to the protein structure is too low to influence the process of the structure formation during fibroin regeneration. No significant absorbance due to the presence of RB19 was found in the FTIR spectra because the

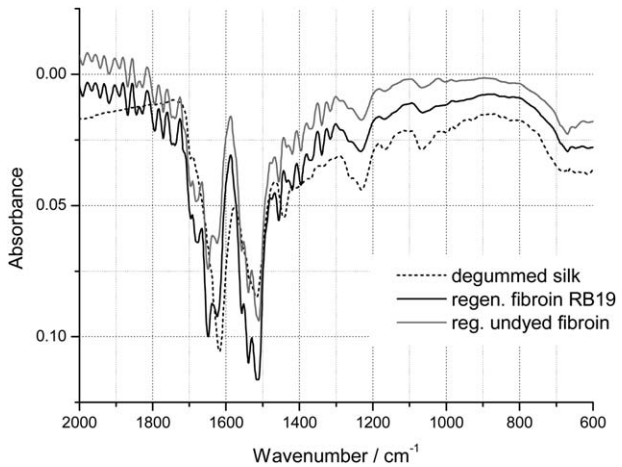

Figure 6. FTIR-ATR analysis of regenerated RB19 dyed fibroin, regenerated undyed fibroin and degummed fibroin.

Table II. CIELab Coordinates and *K/S* Value (590 nm) of CV Fiber Samples after Sorption Experiments with RB19 Labelled Fibroin as a Function of the Amount of Fibroin used in g of 13 wt % Fibroin Solution per 0.5 g Fiber and wt % Fibroin, at pH 3, 60 °C

Temp. °C	pH	Fibroin solution g	Fibroin wt %	L^* ± sd	a^* ± sd	b^* ± sd	*K/S* ± sd
60	3	0.00	0.00	92.94 ± 6.04	−0.21 ± 0.03	2.08 ± 0.65	0.03 ± 0.04
		0.10	2.60	85.91 ± 0.73	−1.9 ± 0.15	−7.30 ± 0.31	0.11 ± 0.01
		0.20	5.20	82.75 ± 1.76	−1.9 ± 0.00	−11.42 ± 0.72	0.18 ± 0.03
		0.30	7.80	81.14 ± 0.99	−1.03 ± 0.07	−11.89 ± 0.16	0.21 ± 0.02
		0.50	13.00	82.57 ± 0.01	−1.47 ± 0.67	−10.46 ± 0.77	0.18 ± 0.01
		0.70	18.20	81.82 ± 2.31	−0.89 ± 0.45	−10.37 ± 2.81	0.18 ± 0.03

concentration of dyestuff remained below the detection limit of the FTIR method.

Sorption Behavior of RB19 Marked Fibroin on Manmade Fibers

When a fibroin solution in CWE is diluted with water, the reduction in Ca-ion concentration should lead to a reduction in solution stability of the dissolved fibroin. In the presence of fibrous material sorption and deposition of fibroin on the fiber surface should occur.

The RB19 labelled fibroin allows the direct monitoring of fibroin sorption/deposition on fibrous material by color measurement of fiber samples and photometry of the residual solution. Three different types of fibers were used. A viscose type fiber (CV) as a representative for a cellulose, polyethylene terephthalate (PES) and polyamide 6.6 (PA) fibers were chosen as important synthetic fibers.

The RB19 dyed fibroin was dissolved in CWE to obtain a 13 wt % fibroin solution. Different amounts of fibroin solution in the range of 0–700 mg were diluted with 100 mL water to obtain the solution for sorption experiments. An amount of 0.5 g of fiber sample then was treated in the solution for 20–24 h. Two temperatures 30 °C and 60 °C were studied. Besides the initial value of pH 5–6 which is near to the isoelectric point of unlabelled fibroin, another series of experiments were performed at a reduced pH of 3, where also the RB 19 marked fibroin protein can be assumed to be positively charged, as also the amino group in the structure of RB 19 will be protonated at this pH (Figure 1). Photos of the treated fiber samples are shown in the supporting information (Supporting Information Figure S2).

The CIELab coordinates and the *K/S* value (590 nm) of the treated CV fiber samples are shown in Table II. The respective results of PES and PA fibers are shown in Tables III and IV, respectively.

As expected, the intensity of the blue color increases with the amount of RB19 labelled fibroin, which can be seen with the increasing value of both the b^* coordinate and the *K/S* value of the stained sample (Figure 7).

The increase in *K/S* value, with the added amount of dyed fibroin, follows an almost linear relationship, indicating that no saturation effects are observed. Screening experiments at pH 5–6 and 30 or 60 °C also resulted in lighter dyeing as the overall process of fibroin destabilization, coagulation and deposition proceeds much slower.

The reduction of pH from the initial value between pH 5–6 to a pH of 3 increases dyestuff deposition on the fiber surface. This can be explained by the destabilization of the fibroin solution at a lower pH, thus leading to higher deposition rate on the fiber surface.[33,34]

Substantial differences in fibroin uptake were found between viscose (as a cellulose fiber) and the two synthetic fibers, polyester, and polyamide. This finding supports the assumption that the mechanism of the fibroin deposition includes sorption effects, as the chemical nature of the sorbent also influences the fibroin layer formation.

The sorption behavior is more clearly visible in the experiments at pH 5–6 and 60 °C, where the solution is less destabilized and the interaction between the fiber surface and protein in the

Table III. CIELab Coordinates and *K/S* Value (590 nm) of PES Fiber Samples after Sorption Experiments with RB19 Labelled Fibroin as a Function of Amount of the Fibroin Used in g of 13 wt % Fibroin Solution per 0.5 g Fiber and wt % Fibroin, at pH 3, 60 °C

Temp. °C	pH	Fibroin solution g	Fibroin wt %	L^* ± sd	a^* ± sd	b^* ± sd	*K/S* ± sd
60	3	0.00	0.00	90.50 ± 5.03	−0.28 ± 0.42	0.30 ± 1.80	0.04 ± 0.04
		0.10	2.60	77.59 ± 5.65	−3.12 ± 0.30	−15.39 ± 1.17	0.37 ± 0.19
		0.20	5.20	73.55 ± 3.31	−2.87 ± 0.23	−20.55 ± 0.53	0.55 ± 0.16
		0.30	7.80	69.08 ± 0.69	−1.61 ± 0.99	−24.37 ± 1.34	0.79 ± 0.09
		0.50	13.00	64.93 ± 4.68	−1.24 ± 0.28	−27.62 ± 2.09	1.16 ± 0.41
		0.70	18.20	63.00 ± 13.72	−0.66 ± 2.54	−26.42 ± 5.94	1.52 ± 1.31

Table IV. CIELab Coordinates and *K/S* Value (590 nm) of PA Fiber Samples after Sorption Experiments with RB19 Labelled Fibroin as Function of Amount of Fibroin used in g of 13 wt % Fibroin Solution per 0.5 g Fiber and wt % Fibroin, pH 3, 60 °C

Temp. °C	pH	Fibroin solution g	Fibroin wt %	$L^* \pm$ sd	$a^* \pm$ sd	$b^* \pm$ sd	$K/S \pm$ sd
60	3	0.00	0.00	94.97 ± 2.71	−0.33 ± 0.18	0.79 ± 0.62	0.01 ± 0.01
		0.10	2.60	73.36 ± 0.71	−3.08 ± 0.40	−24.72 ± 1.36	0.62 ± 0.02
		0.20	5.20	69.18 ± 0.38	−2.60 ± 0.75	−27.67 ± 2.76	0.88 ± 0.06
		0.30	7.80	66.78 ± 0.28	−2.11 ± 0.64	−29.47 ± 2.33	1.07 ± 0.06
		0.50	13.00	64.63 ± 1.34	−1.48 ± 0.35	−31.35± 7.71	1.27 ± 0.08
		0.70	18.20	59.71 ± 2.06	−0.41 ± 2.54	−33.69± 1.73	1.82 ± 0.28

solution determines the fibroin deposition to a higher extent. Distinct differences in color uptake were obtained between viscose, polyester and polyamide, with the highest fibroin sorption on polyamide fibers (Figure 8). The CIELab coordinates and the *K/S* value measured at 590 nm of the fiber samples treated at pH 5–6 are given in the Supporting Information (Tables SIII–SV).

In Figure 9, the absorbance of RB19 fibroin solutions after the sorption experiments (solution S) are shown. As expected, the absorbance increases with the amount of dyestuff used. The reduction in absorbance is more pronounced in the experiments at pH 3. In experiments at pH 5–6 the major part of fibroin remains solubilized. As indicated from the results of the color measurement at pH 5–6, the lowest sorption is detected on viscose fibers thus the highest absorbance is determined for these solutions. At pH 3, a change in the absorbance curves is found for PES and PA fibers as the characteristic curve for RB19 disappears. In the range of 400–700 nm, the absorbance of these solutions is almost independent of wavelength which is an indication of the presence of the dispersed coagulated material, which mainly reduces light intensity through scattering. This explanation is supported by the photographs of the solutions (Supporting Information Figure S3), which show the presence of the dispersed blue coagulate that separates from a clear colorless solution.

From calibration curves with RB19 fibroin solutions, an evaluation of residual RB19 labelled fibroin in the test solutions could be attempted, however due to the instability of the solubilized state and the tendency of the fibroin to coagulate such an evaluation was not undertaken.

The absorbance increased with the amount of dissolved RB19 fibroin solution. For a given solution pH, the highest absorbance was observed for experiments with CV [Figure 9(a,b)]. Higher absorbance was observed for experiments at pH 5–6 compared to experiments at pH 3. In general, higher absorbance of the residual solution was observed for experiments where the color of treated fiber samples was lighter.

Selected samples of treated polyamide fibers and respective reference material were stained with Coomassie Blue G-250 to indicate the presence of proteins on the fiber surface. Thus raw silk, degummed silk, pristine polyamide fibers and treated polyamide fibers (18.2 wt % fibroin at 60 °C, pH 3) were stained with Coomassie Blue G-250 solution. The color of the samples was characterized by the measurement of the color coordinates and the *K/S* value at 610 nm. The results are given in Table V

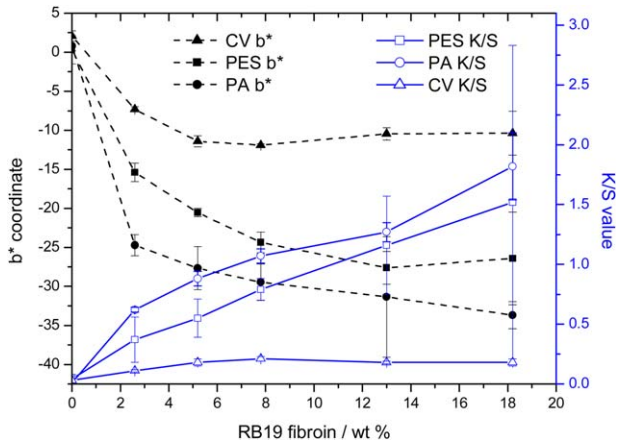

Figure 7. *b**coordinate and *K/S* (590 nm) value of RB19 stained fibers at 60 °C, pH 3, as a function of the amount of RB19 labelled fibroin (error bars indicate standard deviation). [Color figure can be viewed in the online issue, which is available at wileyonlinelibrary.com.]

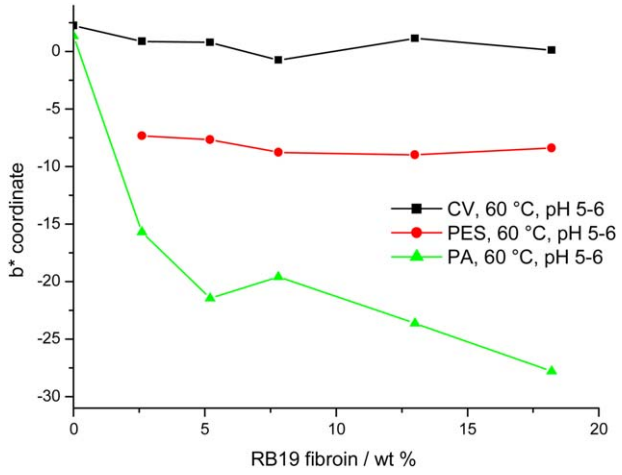

Figure 8. *b**coordinate and *K/S* (590 nm) value of stained fibers at 60 °C, pH 5–6, as a function of the amount of RB19 labelled fibroin. [Color figure can be viewed in the online issue, which is available at wileyonlinelibrary.com.]

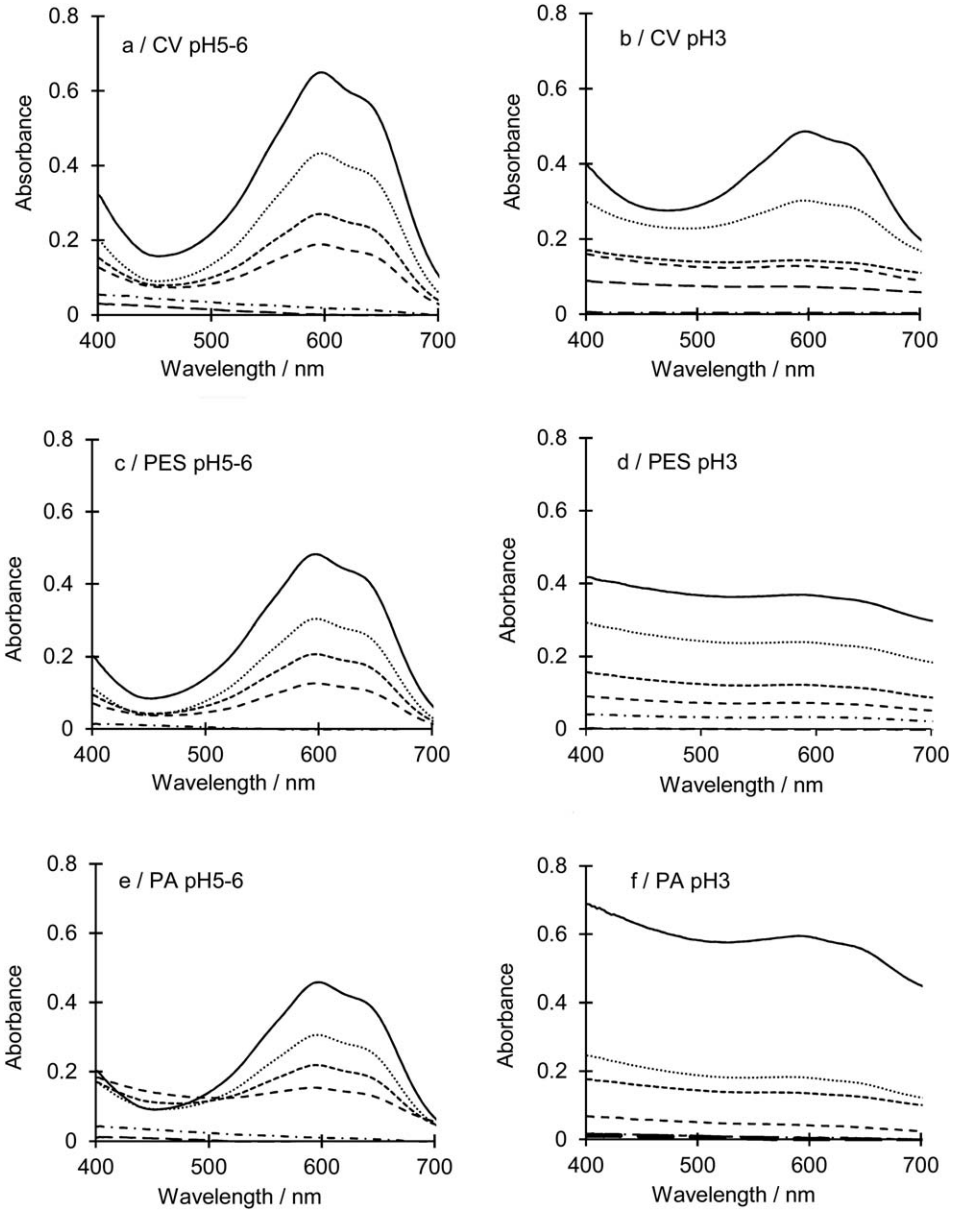

Figure 9. Absorbance spectra of residual solution S at the end of the sorption experiment for different manmade fibers as function of pH and amount of fibroin solution used: (a) CV pH 5–6; (b) CV pH 3; (c) PES pH 5–6; (d) PES pH 3; (e) PA pH 5–6; (f) PA pH 3; (——) 700 mL; (···) 500 mL; (- -) 300 mL; (− −) 200 mL; (- · -) 100 mL; (— —) 0 mL.

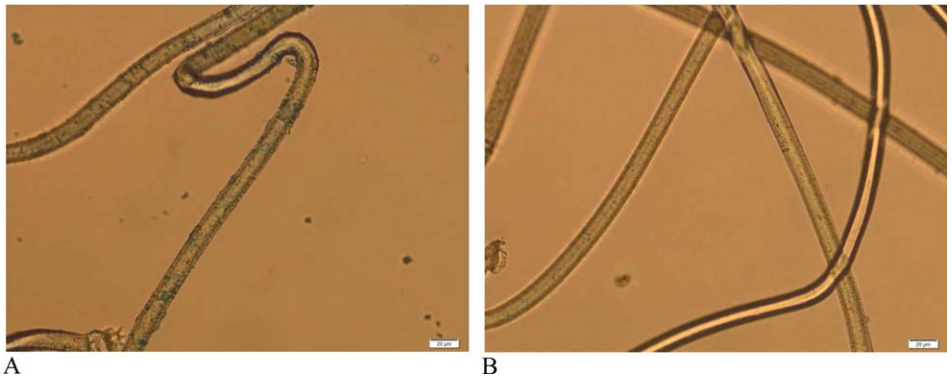

Figure 10. Photographs of Coomassie G-250 stained samples (A) RB19 treated PA fibers (60 °C, pH 3, 18.2 wt % fibroin); (B) pristine PA after staining. [Color figure can be viewed in the online issue, which is available at wileyonlinelibrary.com.]

Table V. CIELab-Color Coordinates and *K/S* (610 nm) Values of Coomassie G-250 Stained Samples (Mean of Three Measurements and Standard Deviation)

Sample	$L^* \pm$ sd	$a^* \pm$ sd	$b^* \pm$ sd	$K/S \pm$ sd
Raw silk	36.13 ± 1.02	−2.46 ± 0.39	−39.24 ± 1.35	15.04 ± 1.13
Degummed silk	47.46 ± 0.57	−5.89 ± 1.03	−41.94 ± 1.37	7.38 ± 0.43
PA	74.69 ± 0.97	−10.96 ± 0.12	−16.91 ± 0.23	0.64 ± 0.05
PA with fibroin	48.38 ± 0.55	−3.94 ± 0.36	−39.56 ± 0.73	5.34 ± 0.29

and photographs are shown in Figure 10. Coomassie Blue G-250 stained protein deposits on the surface of the PA fibers can be seen using a microscope. Photographs of the samples are shown in supporting information (Supporting Information Figure S4).

CONCLUSIONS

Through the chemical attachment of a reactive dye, fibroin can be labelled which then allows a simple observation of the dissolution and regeneration by photometry. Reactive Blue 19 labelled fibroin allowed direct monitoring of the coagulation and sorption of fibroin during the regeneration step in presence of man-made fibers. Dependent on the number of anchor groups present in the reactive dye, crosslinking of the protein structure prevents dissolution in CWE.

Using Reactive Blue 19 labelled fibroin, the darkest staining was obtained with polyamide fibers, followed by polyester fibers and cellulose fibers. This indicates that the mechanism of fibroin coagulation and deposition also includes sorption effects, which are dependent on the properties of the fiber surfaces and at a lower pH. The following factors could be assumed to influence the sorption/deposition mechanism of fibroin on the fiber surface:

- Hydrogen bonding is of minor relevance as for example lowest sorption was observed on the surface of cellulose fibers which exhibits a high number of hydroxyl groups.
- In solution the fibroin macromolecule is present in a random coil structure, thus ionic interactions will be supportive forces for adsorption of regenerated silk on the positively charge polyamide fibers. This effect will be supported by the additional negative charge brought into the fibroin through the bound reactive dye.
- The unexpectedly high sorption of regenerated silk on polyester fibers could be supported by π-bond interactions between the terephthalic acid in PES and the tyrosine in fibroin. As an average silk fibroin contains 13% of tyrosine.[27]

The presence of fibroin on the fiber surface was also proven using staining with the protein reagent Coomassie Blue G-250.

The regeneration of fibroin from dissolved state is of high interest for the development of fibroin coatings for the modification of textile fabrics. The next step in the processing of dyed fibroin will to optimize a regeneration method applicable for the coating of textile substrates with undyed fibroin.

ACKNOWLEDGMENTS

Authors thank OEAD (Austrian agency for international mobility and cooperation in education, science and research) for providing a PhD-scholarship to Ha-Thanh Ngo. Authors thank Ms. Ann Blaylock BSc. for English proofreading.

REFERENCES

1. Padaki, N. V.; Das, B.; Basu, A. In Advances in Silk Science and Technology; Basu, A., Ed.; Woodhead Publishing, UK, **2015**; Chapter 1, p 3.
2. McGrath, K.; Kaplan, D. Protein-Based Materials; Birkhäuser: Boston, **1997**.
3. Murugesh Babu, K. Silk—Processing, Properties and Applications; Woodhead Publishing, UK, **2013**.
4. Vepari, C.; Kaplan, D. L. *Prog. Polym. Sci.* **2007**, *32*, 991.
5. Cao, Y.; Wang, B. *Int. J. Mol. Sci.* **2009**, *10*, 1514.
6. Perrone, G. S.; Leisk, G. G.; Lo, T. J.; Moreau, J. E.; Haas, D. S.; Papenburg, B. J.; Golden, E. B.; Partlow, B. P.; Fox, S. E.; Ibrahim, A. M. S. *Nat. Commun.* **2014**, *5*, 9.
7. Meinel, L.; Betz, O.; Fajardo, R.; Hofmann, S.; Nazarian, A.; Cory, E.; Hilbe, M.; McCool, J.; Langer, R.; Vunjak-Novakovic, G. *Bone* **2006**, *39*, 922.
8. Lin, S. J.; Ibrahim, A. M. S.; Perrone, G. S.; Leisk, G. G.; Lo, T. J.; Moreau, J. E.; Golden, E. B.; Partlow, B. P.; Fox, S. E.; Kaplan, D. L. *Plast. Reconstr. Surg.* **2013**, *132*, 144.
9. Mandal, B. B.; Grinberg, A.; Gil, E. S.; Panilaitis, B.; Kaplan, D. L. *Proc. Natl. Acad. Sci. USA* **2012**, *109*, 7699.
10. Posati, T.; Benfenati, V.; Sagnella, A.; Pistone, A.; Nocchetti, M.; Donnadio, A.; Ruani, G.; Zamboni, R.; Muccini, M. *Biomacromolecules* **2014**, *15*, 158.
11. Dal Pra, I.; Freddi, G.; Minic, J.; Chiarini, A.; Armato, U. *Biomaterials* **2005**, *26*, 1987.
12. Bayraktar, O.; Malay, Ö.; Özgarip, Y.; Batıgün, A. *Eur. J. Pharm. Biopharm.* **2005**, *60*, 373.
13. Silva, N. H. C. S.; Vilela, C.; Marrucho, I. M.; Freire, C. S. R.; Pascoal Neto, C.; Silvestre, A. J. D. *J. Mater. Chem. B* **2014**, *2*, 3715.
14. Sah, M. K.; Pramanik, K. *Int. J. Environ. Sci. Dev.* **2010**, *1*, 404.
15. Durasevic, V.; Machnowski, W.; Kotlinska, A. 4th International Textile, Clothing and Design Conference—Magic World of Textiles, Oct. 5–8, **2008**, Dubrovnik, Croatia.
16. Ajisawa, A. *J. Seric. Sci. Jpn.* **1998**, *67*, 91.

17. Lv, Q.; Cao, C.; Zhang, Y.; Ma, X.; Zhu, H. *J. Appl. Polym. Sci.* **2005**, *96*, 2168.
18. Lv, Q.; Hu, K.; Feng, Q.; Cui, F. *J. Biomed. Mater. Res. A* **2008**, *84*, 198.
19. Deveci, S. S.; Basal, G. *Colloid. Polym. Sci.* **2009**, *287*, 1455.
20. Zheng, Z.; Wei, Y.; Yan, S.; Li, M. *J. Fiber Bioeng. Informatics* **2009**, *2*, 162.
21. Lv, Q.; Cao, C.; Zhang, Y.; Man, X.; Zhu, H. *J. Mater. Sci. Mater. Med.* **2004**, *15*, 1193.
22. Chen, X.; Knight, D. P.; Shao, Z.; Vollrath, F. *Polymer (Guildf)* **2001**, *42*, 9969.
23. Koebley, S. R.; Thorpe, D.; Pang, P.; Chrisochoides, P.; Greving, I.; Vollrath, F.; Schniepp, H. C. *Biomacromolecules* **2015**, *16*, 2796.
24. Lu, Q.; Zhang, B.; Li, M.; Zuo, B.; Kaplan, D. L.; Huang, Y.; Zhu, H. *Biomacromolecules* **2011**, *12*, 1080.
25. Lin, Y.; Xia, X.; Shang, K.; Elia, R.; Huang, W.; Cebe, P.; Leisk, G.; Omenetto, F.; Kaplan, D. L. *Biomacromolecules* **2013**, *14*, 2629.
26. Sohn, S.; Guido, S. P. *Biomacromolecules* **2009**, *10*, 2086.
27. Rath, H. In Lehrbuch der Textilchemie; Springer-Verlag: Berlin Heidelberg, **1972**.
28. Bui, H. M.; Ehrhardt, A.; Bechtold, T. *Cellulose* **2009**, *16*, 27.
29. Ngo, H. T.; Bechtold, T. Analysis of Fibroin Solution in Calcium Chloride/Water/Ethanol Solution as Basis for Direct Regeneration, submitted.
30. Dubey, P.; Murab, S.; Karmakar, S.; Chowdhury, P. K.; Ghosh, S. *Biomacromolecules* **2015**, *16*, 3936.
31. Hu, X.; Kaplan, D.; Cebe, P. *Macromolecules* **2006**, *39*, 6161.
32. Zhang, C.; Song, D.; Lu, Q.; Hu, X.; Kaplan, D. L.; Zhu, H. *Biomacromolecules* **2012**, *13*, 2148.
33. Kim, U. J.; Park, J.; Li, C.; Jin, H. J.; Valluzzi, R.; Kaplan, D. L. *Biomacromolecules* **2004**, *5*, 786.
34. Dang, Q.; Lu, S.; Yu, S.; Sun, P.; Yuan, Z. *Biomacromolecules* **2010**, *11*, 1796.